Talanta 270 (2024) 125626

Contents lists available at ScienceDirect

Talanta

journal homepage: www.elsevier.com/locate/talanta

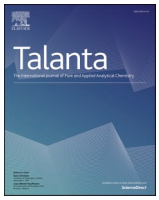

Synthesis of in-situ magnetized MOF-cellulose membranes for high-efficiency enrichment of diamide insecticides in vegetables and determination by LC-MS/MS

Yuning Wang, Jingkang Li, Pinyi Ma, Dejiang Gao **, Daqian Song *

College of Chemistry, Jilin Province Research Center for Engineering and Technology of Spectral Analytical Instruments, Jilin University, Qianjin Street, 2699, Changchun, China

ARTICLE INFO

Handling editor: Kin-ichi Tsunoda

Keywords:
Metal-organic frameworks (MOFs)
In-situ magnetized
Cellulose membranes
Diamide insecticides
Vegetables

ABSTRACT

This study presents a novel, eco-friendly composite adsorbent material designed for the magnetic solid-phase extraction of diamide insecticides from vegetable samples. The membrane, denoted as Fe-MMm, was incorporated with a cellulose framework embedded with Metal-Organic Frameworks (MOFs) and Multi-Walled Carbon Nanotubes (MWCNTs) magnetized with Fe_3O_4. This innovative material streamlined the conventional solid-phase extraction process, simplifying the sample pre-treatment. By combining it with liquid chromatography tandem mass spectrometry (LC-MS/MS), the method achieves significantly enhanced extraction efficiency through systematic optimization of experimental parameters, including adsorbent selection, pH, ionic strength, adsorption time, and elution time. The method had a wide linear range of 0.1–1000 ng/mL and an exceptionally low detection limit ranging from 0.023 to 0.035 ng/mL. The successful identification of diamide insecticides in vegetable samples underscores the potential of Fe-MMm as a robust material for sample pretreatment in analytical applications.

1. Introduction

In agricultural practices, a wide variety of pesticides are employed to control pests and weeds. However, the presence of pesticide residues in commonly consumed vegetables poses potential risks to human health when concentrations exceed the regulatory limits [1]. Among these pesticides, diamide insecticides, such as Tolfenpyrad (TORAC), Flubendiamide (FBD), Cyantraniliprole (CNAP), Cyclaniliprole (CYCP), and Tetrachlorantraniliprole (TCAP), have garnered increasing attention [2] (Fig. 1). These insecticides exhibit high selectivity towards lepidopteran pests by targeting their ryanodine receptors and disrupting their calcium homeostasis, which ultimately leads to their demise [3]. Despite the favorable safety to non-target organisms of these insecticides [4], their widespread use has raised concerns due to their potential ecological and human health risks. For instance, since 2018, the use of FBD has been prohibited in China for rice cultivation owing to its detrimental impact on invertebrates and aquatic ecosystems [2]. The European Food Safety Authority has established an allowable daily intake of FBD at 0.017 mg/(kg·d) [5]. Moreover, the Environmental Protection Agency (EPA) has issued the regulation 2020–27906 after conducting a comprehensive risk assessment of toxicity, dietary exposure, and effects on infants and young children and considered FBD and CNAP safe for some foods at a residue limit of 0.01 mg/(kg·d). Consequently, there is an urgent need for the development of highly sensitive analysis and detection techniques for trace amounts of diamide insecticides.

Addressing the challenges associated with the detection of diamide insecticides in complex matrices often requires sample pre-processing Conventional methods for this purpose include liquid-liquid extraction [6], QuEChERS (Quick, Easy, Cheap, Effective, Rugged, and Safe) [7], and solid-phase extraction (SPE) [8]. Some researchers have adapted the QuEChERS methodology to develop targeted assays for detecting diamide insecticides in less complex matrices [9]. For instance, specific protocols have been established to detect chlorphenamide in grapes, cabbage, and cauliflower [10,11]. In 2020, Tian et al. proposed a comprehensive method for simultaneous detection of five different diamide insecticides by leveraging QuEChERS technology [12]. Although QuEChERS method offers a robust and straightforward approach, SPE is more advantageous due to several reasons, including

* Corresponding author.
** Corresponding author.
E-mail addresses: gaodejiang@jlu.edu.cn (D. Gao), songdq@jlu.edu.cn (D. Song).

https://doi.org/10.1016/j.talanta.2024.125626
Received 17 October 2023; Received in revised form 30 December 2023; Accepted 3 January 2024
Available online 7 January 2024

reduced consumption of organic solvents, enhanced repeatability, greater analyte specificity, and more simplified operational procedures. Nevertheless, traditional SPE methods face with some challenges, particularly in terms of enrichment capacity and the selection of suitable adsorbents.

Metal-organic frameworks (MOFs) are a class of porous coordination polymers comprising organic ligands and inorganic metal ions. These materials are renowned for their exceptional specific surface areas and porosity, making them ideal candidates for separation and adsorption applications [13]. Typically, MOFs utilize organic ligands this can also be "that can be categorized into two board groups: carboxylic acids (such as terephthalic acid) and neutral compounds containing nitrogen-based heterocycles (such as 2-methylimidazole). Extant literature suggests that many MOFs contain hydrophobic channels that can establish robust π-π interactions and hydrophobic interactions with diamide pesticides and other aromatic compounds [14,15]. As a result, they are frequently employed as separation and enrichment materials for pesticide detection [16]. However, because MOFs are susceptible to dispersion in aqueous media, their direct use in solid-phase extraction increases the risk of MOF loss during solid-liquid separation, which in turn leads to significant experimental errors, poor reproducibility, and methodological instability.

To circumvent the limitations associated with the direct use of MOFs in solid-liquid separation, our study introduced cellulose as a carrier matrix. Cellulose-based membranes have been extensively used as filtration media, and researchers have further modified their surfaces to enhance their selective adsorption capacities for solid-phase extraction [17]. By utilizing a vacuum filtration technique [18], we uniformly embedded a composite adsorbent, MOFs/MWCNTs@Fe_3O_4, into the cellulose framework. This engineering approach yielded a membrane material that was endowed with robust mechanical stability and reusability. Subsequently, we employed this cellulose-based composite material as a separation and enrichment medium for the pre-treatment of vegetable samples, specifically using magnetic solid-phase extraction (MSPE). When use in conjunction with high-performance liquid chromatography-tandem mass spectrometry (HPLC-MS/MS), this novel method is a highly sensitive, stable, and reproducible analytical protocol for the detection of trace concentrations of diamide insecticides in vegetable samples.

2. Materials and methods

2.1. Reagents and instruments

Information of reagents and materials can be found in Supporting Information.

2.2. Synthesis of MOFs

MIL-101(Cr)-NH_2 was synthesized following established protocols reported in the literature [19]. Specifically, 800 mg of $Cr(NO_3)_3{\cdot}9H_2O$ and 360 mg of 2-aminoterephthalic acid were dispersed in 20 mL of deionized water. The mixture was transferred to a 30 mL Teflon-lined stainless steel autoclave and subjected to a hydrothermal reaction at 150 °C for 10 h. After the autoclave was cooled to room temperature, the resulting precipitate was isolated via centrifugation. The collected solid was then sequentially washed with dimethylformamide (DMF) and methanol to yield a green-colored product. Additional MOFs were synthesized using similar methods, the details of which are provided in Supporting Information.

2.3. Synthesis of MWCNTs@Fe_3O_4

The synthesis of MWCNTs@Fe_3O_4 is as follows: Initially, 5 g of $FeCl_3{\cdot}6H_2O$ and 12.5 g of NaOAc were sequentially dissolved in 100 mL of ethylene glycol. Subsequently, 3.3 g of PEG and 1 g of MWCNT-COOH were added to the solution. The mixture was agitated for 30 min at room temperature until homogeneous. The dispersion was then divided into five aliquots with an equal volume and transferred to stainless steel autoclaves lined with polytetrafluoroethylene. The autoclaves were subjected to a hydrothermal treatment at 200 °C for 10 h. Upon completion, the resulting product was isolated via centrifugation, washed with ethanol, and then dried overnight.

2.4. Synthesis of Fe-MMm

A composite mixture was prepared by combining 50 mg of MOFs and 50 mg of magnetic carbon nanotubes in a beaker, to which 50 mL of water was added. The mixture was subjected to in-situ magnetization via ultrasonic treatment for 10 min. In our study, we carefully calibrated the ultrasonic power to ensure that the structural integrity of MOFs was not compromised. The ultrasonic treatment process may contribute to enhancing certain properties of MOFs, such as increasing surface area or

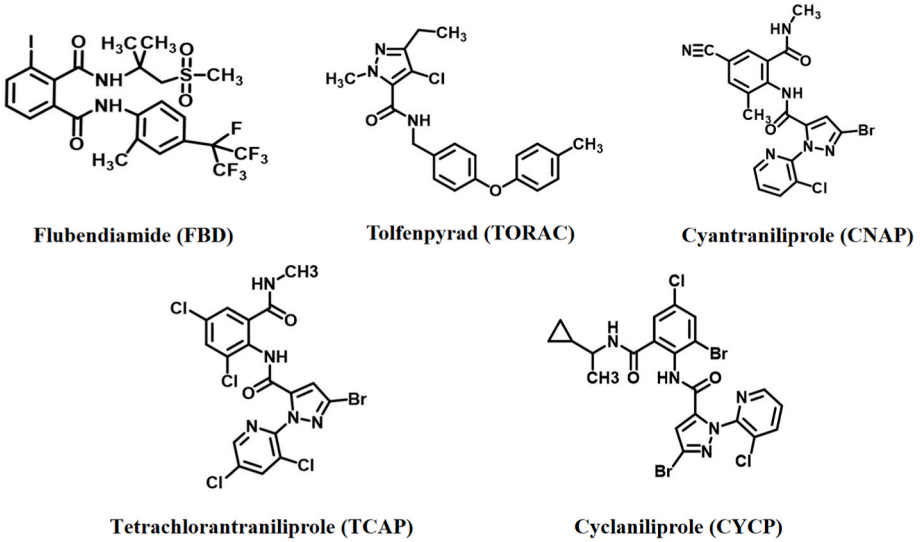

Fig. 1. Molecular structures of five diamide insecticides.

improving pore accessibility, thereby positively affecting the adsorption process. Subsequently, 10 g of MFC dispersion was introduced, and the mixture was uniformly dispersed by ultrasonic agitation. The membrane was then fabricated using a vacuum filtration method. After the filtration process was complete, the membrane frame was carefully removed from the Büchner funnel and allowed to dry at room temperature for 12 h. To expedite the drying process, Whatman filter papers were replaced every 2 h. Fully dried membrane was subsequently cut into small disks with a fixed diameter of 15 mm using a precision piercing machine. The specific details of this procedure are illustrated in Fig. S1.

2.5. MSPE procedure

The adsorption was enhanced by the use of constant temperature and constant-speed shaking to allow for efficient solid-liquid separation with the aid of an external magnetic field. To fine-tune the experimental conditions, a range of parameters, including the choice of adsorbent, solution pH, salt concentration, adsorption duration, elution solvent type and volume, and elution time, were systematically optimized. The extraction process is depicted in Fig. 2.

Initially, a 3.5 mL aliquot of sample solution with a concentration of 10 ng/mL was introduced into a 5 mL centrifuge tube. Next, a piece of Fe-MMm was added into the sample solution, and the mixture was continuously shaken at 1000 rpm for 30 min at 28 °C. Subsequently, the supernatant was discarded, and the adsorbed amine compounds were eluted using 3 mL of acetonitrile by agitating at 1000 rpm for 30 min. The eluate was then dried under a gentle nitrogen stream at 45 °C and reconstituted in 100 μL of chromatography-grade acetonitrile. The final solution was then filtered through a 0.22 μm nylon membrane filter before being subjected to analysis by an HPLC-MS/MS system.

3. Results and discussion

3.1. Characterization

Specific peaks in the Fourier transform infrared spectroscopy (FT-IR) spectra serve as indicators for successful synthesis. In Fig. 3(A–a) peaks at 1339 cm^{-1} and 1250 cm^{-1} can be ascribed to the C-N vibrational modes of aromatic amines. Additional peaks at 3415 cm^{-1} and 1622 cm^{-1} are corresponded to the stretching vibrations of -NH_2 and the bending vibrations of N-H, respectively [20]. The peak at 1399 cm^{-1} is attributed to the stretching vibrations of -(O-C-O)-, while that at 577 cm^{-1} can be assigned to the stretching vibrations of Cr-O [21]. These peaks confirm the successful coordination between metal clusters and carboxyl group of 2-aminoterephthalic acid and validate the successful synthesis of the target sample. In Fig. 3(A and b), the peak at 1638 cm^{-1} is indicative of the stretching vibrations of C=O. Two bands near 3450 cm^{-1} and 586 cm^{-1} can be assigned to the bending vibrations of O-H in adsorbed water and the Fe-O vibrations in Fe_3O_4, respectively [22]. These peaks confirm the successful attachment of Fe_3O_4 onto the surface of MWCNTs and further validate the successful synthesis of the target sample. In Fig. 3(B–a), distinct peaks corresponding to MFC were observed, including the peak at 3430 cm^{-1} indicating the stretching vibrations of O-H, and the peak at 2900 cm^{-1} representing the symmetrical stretching of C-H in methylene. Furthermore, the absorbance at 1058 cm^{-1} is primarily attributed to the C-O stretching of cellulose [23]. No significant changes were observed in the infrared spectra of Fe-MMm before and after adsorption, as depicted in Fig. 3(B–b) and Fig. 3(B and c). The absorption peaks mentioned above also appear in Fe-MMm (Fig. 3(A)). The distinctive peaks corresponding to MFC, such as the stretching vibrations of O-H at 3430 cm^{-1} and the symmetrical stretching of C-H in methylene at 2900 cm^{-1}, were clearly evident in the spectra. This indicates the successful synthesis of Fe-MMm.

Additionally, the specific surface areas and pore sizes of the synthesized materials were examined based on N_2 adsorption-desorption isotherms. As shown in Table S2, MIL-101(Cr)-NH_2 had a specific surface area of 1599.1897 m^2/g and an average pore size of 4.51947 nm, exhibiting the characteristic type IV adsorption isotherm [21]. At lower relative pressures (p/p_0), the desorption curve was closely paralleled to the adsorption curve, as depicted in Fig. 3(C). The observed hysteresis loop at higher p/p_0 values indicates the presence of mesopores, which can provide additional adsorption sites for diamine insecticides.

Conversely, MWCNT@Fe_3O_4 had a specific surface area of 50.5944 m^2/g and an average pore size of 34.00786 nm. Fig. 3(D) presents the magnetization curves for MWCNTs@Fe_3O_4 and Fe-MMm obtained via vibrating sample magnetometry (VSM) at room temperature at a magnetic field range of -20 KOe to 20 KOe. Notably, as indicated by the absence of hysteresis, these materials exhibited superparamagnetic behavior [24]. The saturation magnetization (Ms) decreased from 33.464 emu·g^{-1} to 14.296 emu·g^{-1} upon the preparation of Fe-MMm. Despite this reduction, the magnetization remains sufficient for practical applications [25]. Additionally, these materials can be rapidly collected using an external magnet within only 2 s.

Fig. S2(A)and (B) present the X-ray diffraction (XRD) spectra of the synthesized materials, showing the characteristic peaks that align with those reported in the literature [22,25]. Fig. 4(A) and (B) illustrate the structures of the cellulose-based membrane and MIL-101(Cr)-NH_2, respectively. Fig. 4(C) shows a scanning electron microscope (SEM) image vividly illustrating the integration of MIL-101(Cr)-NH_2 and MWCNTs@Fe_3O_4 in the cellulose paper matrix. The fibrous architecture

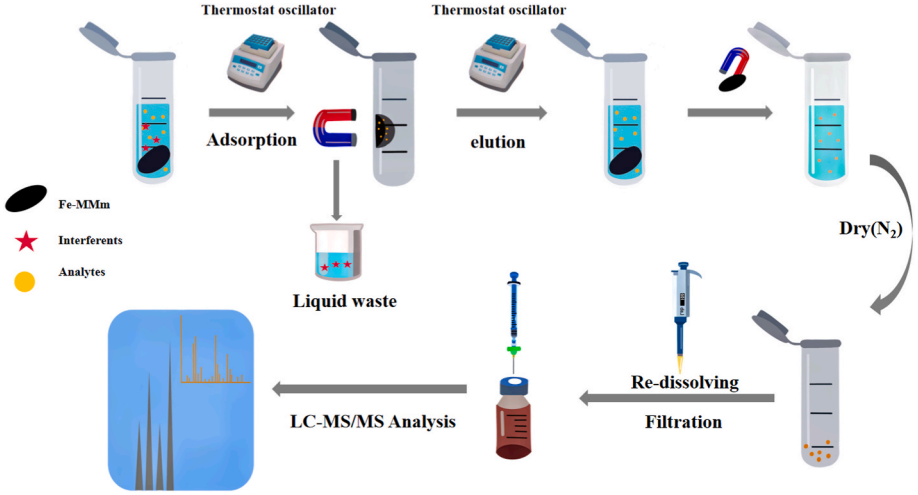

Fig. 2. Schematic diagram of MSPE and analysis process.

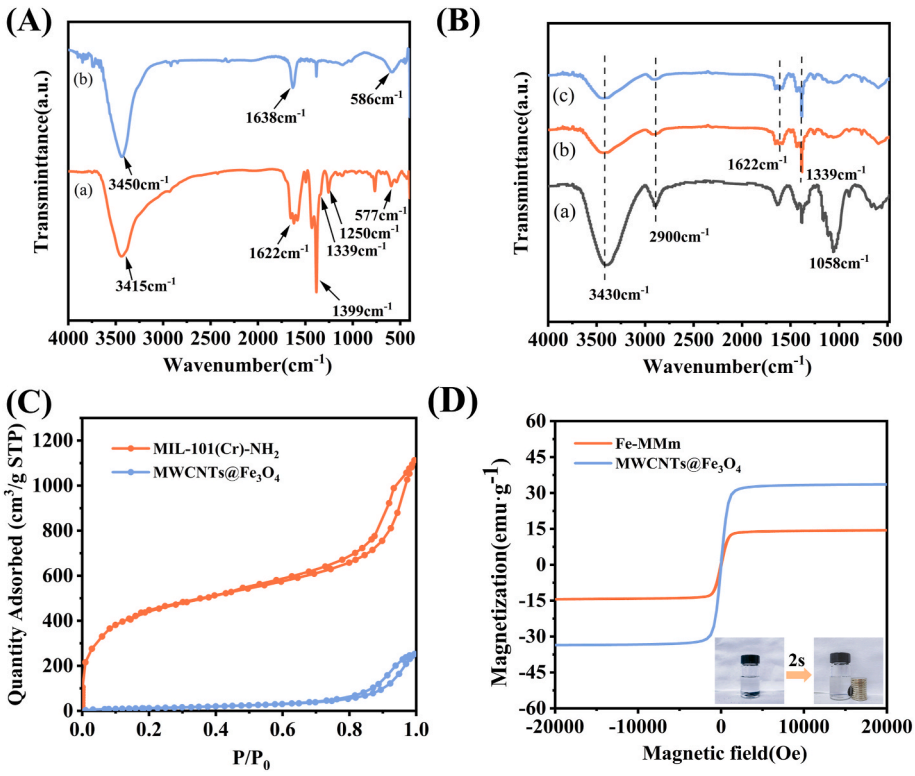

Fig. 3. (A) FT-IR spectra: (a) MIL-101(Cr)-NH_2 and (b) MWCNT@Fe_3O_4, (B) FT-IR spectra: (a) MFC, (b) Before Fe-MMm adsorption and (c) After Fe-MMm adsorption, (C) N_2 adsorption-desorption isotherms, (D) Magnetic curves (298 K).

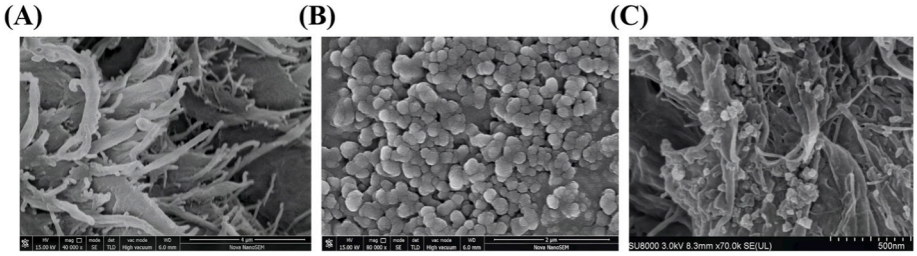

Fig. 4. (A) SEM image of MFC, (B) SEM image of MIL-101(Cr)-NH_2, (C) SEM image of Fe-MMm.

of the cellulose paper was visibly adorned with numerous fine particles adhering to its framework.

Furthermore, Fig. S3 depicts the elemental composition obtained by X-ray photoelectron spectroscopy (XPS) analysis. The full-scan XPS spectra confirmed the presence of Cr, C, N, and O elements in MIL-101 (Cr)-NH_2 and the presence of Cr, C, N, O, and Fe elements in Fe-MMm. Fig. S4 shows XPS spectra of MIL-101(Cr)-NH_2 and Fe-MMm with respect to Cr and N. The Cr 2p XPS spectrum exhibits two characteristic peaks at 577.9 eV and 587.2 eV, indicating the presence of trivalent chromium and Cr-O bonds. The N 1s XPS spectrum displays a peak at 400.1 eV, which corresponds to the characteristic peak of aromatic amines [26].

In conclusion, we successfully synthesized MIL-101(Cr)-NH_2 and MWCNTs@Fe_3O_4 and incorporated them into a cellulose paper matrix. Comprehensive characterization by FT-IR, XRD, SEM, VSM and XPS techniques validated the structural and compositional integrity of the synthesized materials. The FT-IR spectra confirmed the presence of specific functional groups, while the XRD patterns aligned with those reported in the literature, confirming the crystalline nature of the materials. The SEM images revealed a well-integrated microstructure, and XPS analysis further corroborated the elemental composition and specific chemical bonds. Additional assessments, including N_2 adsorption-desorption isotherms and magnetization curves, provided valuable insights into surface areas, pore sizes, and magnetic properties of the materials.

3.2. Optimization of the proposed procedure

3.2.1. Selection of adsorbent materials

In the evaluation of suitability of various metal-organic frameworks (MOFs) for the enrichment of diamide insecticides, we synthesized Fe-MMm membranes using six different MOFs: MIL-68(Al), HKUST-1 (Cu), MIL-101(Cr), MIL-101(Cr)-NH_2, MIL-68(Al)-NH_2 and ZIF-8(Zn). These MOFs were selected based on their aqueous and acidic stability, expansive surface area, and ease of synthesis (Figs. S5–S9).

Fig. S10(A) compares the performance of the six membranes under identical enrichment conditions, which were: a 3.5 mL sample of 10 ng/mL insecticide mixture, 30 min of enrichment time, pH 7, no addition of NaCl, 3 mL of acetonitrile as the elution solvent, and 30 min of elution time. Experimental data indicated that all six membranes could adsorb the insecticides. Notably, the adsorption efficacy of Fe-MMm membrane synthesized with MIL-101(Cr)-NH_2 outperformed that of other membranes. Although MIL-101(Cr) and MIL-101(Cr)-NH_2 shared the same metal ions, they differ in functional groups. MIL-101(Cr)-NH_2

containing -NH_2 groups had higher hydrophilicity compared to its non-functionalized counterpart. Similarly, MIL-68(Al)-NH_2 had greater hydrophilicity than MIL-68(Al). HKUST-1(Cu) and ZIF-8(Zn) led to lower relative recoveries.

There are several factors contributing to the superior performance of MIL-101(Cr)-NH_2. First, its large specific surface area enables higher adsorption capacity at equivalent material dosages. Second, under neutral conditions, the -NH_3^+ groups in MIL-101(Cr)-NH_2 can form hydrogen bonds with the C=O functional groups in diamide insecticides, thereby allowing for enhanced adsorption. This is supported by significant π-π interactions between the conjugated π bonds in the target analytes and the π bonds in MIL-101(Cr)-NH_2. Lastly, MOFs with smaller surface areas and pore sizes are less effective due to the incomplete release of analytes; their small pores can trap analytes, thereby hindering their elution. In contrast, the larger pore size of MIL-101(Cr)-NH_2 allows for efficient adsorption and complete release of the target insecticides. Consequently, Fe-MMm synthesized with MIL-101(Cr)-NH_2 was selected as an adsorbent in subsequent optimization experiments.

3.2.2. Selection of pH

Solution pH is a critical parameter that influences multiple facets of the extraction process, including the surface charge of adsorbent, the chemical structure of analytes, and the overall extraction efficiency. Extreme pH levels can compromise the structural integrity of most MOFs, in turn diminishing their extraction capacity. Specifically, high pH levels can cause MOF degradation, while low pH levels may induce electrostatic repulsion due to altered surface charges, which can consequently lead to lower adsorption efficiency.

To systematically assess the impact of pH on extraction recovery, we conducted experiments at a pH range of 3–11, adjusted using NaOH and HCl. The results depicted in Fig. 5(A) indicate that the optimal recovery was achieved at a neutral pH (pH 7). At a pH range of 5–8, the recovery rate percentage (RR%) remained relatively stable. However, the RR% significantly declined at higher pH values ranging from 9 to 11. It is worth noting that while most MOFs could generally maintain their structural stability in acidic and neutral conditions, those synthesized using 2-aminoterephthalic acid as a ligand were susceptible to decomposition under alkaline conditions. Therefore, subsequent experiments to optimize the adsorption efficiency were conducted under neutral conditions (pH 7).

3.2.3. Selection of salt concentration

The addition of salt can induce a salting-out effect that reduces the solubility of target analytes in a sample solution, which in turn affects the extraction efficiency. To elucidate the influence of salt concentration on the extraction recovery of diamide insecticides, we conducted experiments using NaCl at varying concentrations, ranging from 0% to 10% (w/v), while maintaining other experimental conditions.

As illustrated in Fig. 5(B), the presence of NaCl caused the extraction recovery of all tested diamide insecticides to significantly decline. The reduction in efficiency can be attributed primarily to the increased solution viscosity at elevated salt concentrations, which reduces the diffusion rate of analytes from the aqueous phase to the adsorbent surface [27]. Furthermore, the presence of NaCl, which is non-volatile salt, is incompatible with LC-MS/MS detection methods. Consequently, NaCl was excluded from the final adsorption experiments conducted to optimize extraction efficiency in order to ensure compatibility with analytical detection methods.

3.2.4. Selection of adsorption time

To optimize the adsorption time during the extraction of diamide insecticides, we conducted a series of experiments for varying durations: 1, 3, 6, 9, 12, 15, 18, and 21 min. Fig. 5(C) reveals a significant increase in the signals of all analytes after only 9 min, highlighting the rapid adsorption rates of MIL-101(Cr)-NH_2. This rapid adsorption can be attributed to the large specific surface area and abundant active sites of the material, which allow for the strong interactions with the analytes and the expedition of adsorption equilibrium. The use of a constant-temperature oscillator further enhanced the effective collisions between the adsorbent and analytes, allowing for rapid adsorption. For

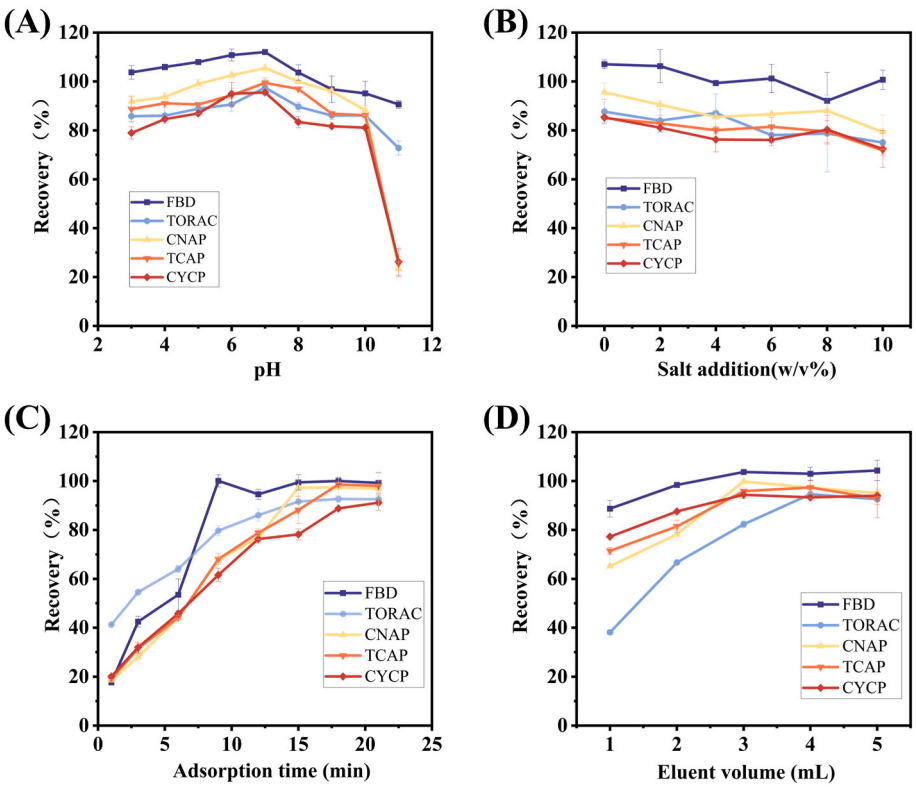

Fig. 5. Optimization of experimental conditions: (A) sample pH, (B) salt concentration, (C) adsorption time, and (D) eluent volume.

durations beyond 18 min, significant changes in the signal intensity were not observed, suggesting that the adsorption equilibrium had been reached. The plateau of the signal intensity is likely due to the saturation of available adsorption sites and the establishment of equilibrium between the adsorption and desorption processes. Based on these findings, 18 min was selected as the optimal adsorption time to allow for both rapid and efficient extraction of the target analytes.

3.2.5. Effects of elution condition

The choice and volume of an elution solvent are critical factors that influence the recovery of adsorbed analytes. Given the varying polarities of the target analytes, we evaluated the elution efficacy of multiple solvents, namely isopropanol, n-hexane, ethyl acetate, methanol, acetonitrile, and dichloromethane. As illustrated in Fig. S10(B), the extraction recoveries using acetonitrile were highest, followed by those using methanol and ethyl acetate, and those using n-hexane were lowest. Consequently, acetonitrile was selected as the elution solvent in subsequent experiments. We further examine the effect of elution solvent volumes from 1 mL to 5 mL. Fig. 5(D) shows that the extraction recovery improved as the volume was increased from 1 mL to 3 mL, but plateaued at higher volumes. To maximize the extraction efficiency while minimizing both cost and solvent waste, an elution volume of 3 mL was chosen for subsequent experiments. The duration of vortex oscillation is another crucial parameter in sample pretreatment, as it directly impacts the extraction recovery. Our investigation into varying elution times, ranging from 1 to 18 min, revealed that the extraction recovery increased up to 9 min and then plateaued (Fig. S11). Therefore, an elution time of 9 min was adopted in subsequent experiments.

3.3. Evaluation of extraction method

3.3.1. Linearity and sensitivity

To validate the efficacy of our proposed extraction method under the optimized conditions, key performance metrics were assessed. As summarized in Table 1, all five diamide insecticides demonstrated a broad linear range at concentrations spanning from 0.1 to 1000 ng/mL. The determination coefficients (R^2) ranged from 0.995 to 0.997, which are indicative of excellent linearity. The detection limits, defined by a signal-to-noise ratio (S/N) of 3, were between 0.023 and 0.035 ng/mL. These data highlight the high sensitivity of our method to diamide insecticides. Compared to those of commercial solid-phase extraction columns and other alternative methods, the detection sensitivity of our approach was higher by 2–3 orders of magnitude and the linear dynamic range was also wider.

3.3.2. Enrichment factor

To assess the effectiveness of the extraction method, the enrichment factor (EF) was computed using the formula:

$$EF = C_{or} / C_{aq}$$

In this formula, C_{aq} denotes the concentration of the analyte in the sample solution, while C_{or} represents the concentration of the analyte in the final organic solvent. The resulting EF values for FBD, TORAC, CNAP, TCAP, and CYCP were determined as 16.1, 15.3, 12.7, 13.5, and 11.8, respectively.

3.3.3. Precision

To assess the precision of our method, we evaluated both intra-day and inter-day precision at an insecticide concentration of 1 ng/mL. The intra-day precision was determined over a single day, while the inter-day precision was assessed over a period of six consecutive days. As presented in Table 1, the relative recoveries (RR%) of five diamide insecticides obtained during intra-day experiments ranged from 94.6% to 106.8%, whereas those obtained during inter-day experiments ranged from 95.3% to 105.3%. The intra-day precision varied between 5.7% and 8.2%, and the inter-day precision ranged from 4.3% to 9.5%. These results attest to the excellent precision of the proposed method.

3.3.4. Reusability

To further underscore the advantages of our novel adsorbent material, we conducted reusability tests. The data obtained after 10 repeated cycles are presented in Fig. S12. The results indicated minimal performance variation across the cycles, affirming that the material has excellent reusability. During the 10 cycles, the specific data for the recovery of Fe-MMm can be found in Table S3.

3.4. Application in real samples

To evaluate the applicability of our method in real-world scenarios, we applied it to five types of leafy green vegetables: Chinese kale, rapeseed, baby bok choy, Chinese cabbage, and spinach. The samples were purchased from a local supermarket in Changchun, China. Initially, 10 g of each vegetable sample was homogenized and blended with 4 mL of methanol. The mixture underwent ultrasonic vortexing for 10 min, followed by high-speed centrifugation. The supernatant was then collected and evaporated to dryness under a nitrogen stream. To prepare a test sample, each dried sample was reconstituted in 30 μL of acetonitrile and 3.5 mL of ultrapure water. Five diamine insecticides were spiked into these samples at concentrations of 1 ng/mL, 10 ng/mL and 100 ng/mL, and recovery experiments were conducted following the procedures outlined in Section 2.5. The results summarized in Table S4 revealed positive detections of FBD in two samples and TORAC in one sample. The relative recovery rates (RR%) for all tested diamine insecticides ranged from 84.3% to 108.1%. The relative standard deviation of less than 9.1% indicated the robustness and reliability of our method in analysis of real samples.

3.5. Comparison with published methods

In the present study, a novel extraction method was proposed and optimized. A comparative analysis between the performance metrics of this MSPE extraction approach and those reported in the literature is detailed in Table S5. Our method offers several advantages over traditional solid-phase extraction techniques. It simplifies the extraction process due to the incorporation of MSPE. Additionally, the use of innovative magnetic cellulose nanocomposite membrane eliminates the need for centrifugation, leading to convenience and enhanced efficiency. Its high recovery rates and excellent stability are maintained, as evidenced by its high relative recovery rates and low relative standard deviations. It is evident that the proposed method is a robust and reliable option for the extraction and quantification of diamine insecticides.

Table 1
Analytical performance of the present method.

Analyte	LDR (ng/mL)	Regression equation	R^2	LOD (ng/mL)	Intra-day (n = 6)		Inter-day (n = 6)	
					RR (%)	RSD (%)	RR (%)	RSD (%)
FBD	0.1–1000	y = 12890.82x+1644.17	0.997	0.035	103.4	8.2	98.6	4.3
TORAC	0.1–1000	y = 81840.08x+6767.14	0.995	0.023	106.8	6.4	105.3	7.2
CNAP	0.1–1000	y = 16212.22x-200.27	0.996	0.031	94.6	5.7	100.1	6.2
TCAP	0.1–1000	y = 10676.41x+157.61	0.995	0.032	100.6	7.5	95.3	5.9
CYCP	0.1–1000	y = 8503.64x-3.66	0.995	0.032	98.2	7.9	99.2	9.5

4. Conclusion

In this investigation, we synthesized six distinct Fe-MMm materials via a vacuum filtration technique and employed them in the sample pretreatment step. Our data conclusively indicated that Fe-MMm materials had exceptional adsorptive capabilities for all five diamide insecticides including FBD,TORAC, CNAP, CYCP, and TCAP, under study. Comprehensive material characterization by SEM, XPS, XRD, FT-IR, VSM, and BET adsorption isotherms corroborated the unique structural and physicochemical attributes of the materials. The integration of thin films into the solid-liquid separation stage eliminated the necessity for centrifugation, thereby enhancing the separation efficiency, even after multiple usages. The proposed methodology also had ultra-high sensitivity, wide linear range, and high robustness and repeatability. The detection limits were remarkably low, 0.023–0.035 ng/mL, which outperformed those of the existing techniques by two to three orders of magnitude. This study substantiates the potential of our novel magnetic cellulose nanomaterial composite film in selective adsorption of trace-level diamide insecticides in vegetable matrices, offering innovative avenues for the analytical detection of insecticides in vegetables.

CRediT authorship contribution statement

Yuning Wang: Writing - original draft, Validation, Software, Methodology, Investigation, Data curation, Conceptualization. **Jingkang Li:** Writing - review & editing, Software, Investigation, Formal analysis. **Pinyi Ma:** Writing - review & editing, Software, Data curation, Conceptualization. **Dejiang Gao:** Supervision, Resources, Project administration, Funding acquisition. **Daqian Song:** Project administration, Funding acquisition, Data curation, Conceptualization.

Declaration of competing interest

The authors declare that they have no known competing financial interests or personal relationships that could have appeared to influence the work reported in this paper.

Data availability

Data will be made available on request.

Acknowledgements

This work was supported by the Science and Technology Developing Foundation of Jilin Province of China (Nos. 20230204116YY, 20230505010ZP and YDZJ202302CXJD031).

Appendix A. Supplementary data

Supplementary data to this article can be found online at https://doi.org/10.1016/j.talanta.2024.125626.

References

[1] A.M. Ares, S. Valverde, J.L. Bernal, L. Toribio, M.J. Nozal, J. Bernal, Determination of flubendiamide in honey at trace levels by using solid phase extraction and liquid chromatography coupled to quadrupole time-of-flight mass spectrometry, Food Chem. 232 (2017) 169–176, https://doi.org/10.1016/j.foodchem.2017.03.162.

[2] P. Wang, X. Liu, X. Wu, J. Xu, F. Dong, Y. Zheng, Evaluation of biochars in reducing the bioavailability of flubendiamide in water/sediment using passive sampling with polyoxymethylene, J. Hazard Mater. 344 (2018) 1000–1006, https://doi.org/10.1016/j.jhazmat.2017.12.003.

[3] M. Paramasivam, C. Selvi, S. Chandrasekaran, Persistence and dissipation of flubendiamide and its risk assessment on gherkin (Cucumis anguria L.), Environ. Monit. Assess. 186 (8) (2014) 4881–4887, https://doi.org/10.1007/s10661-014-3745-2.

[4] K.K. Sharma, I. Mukherjee, B. Singh, S.K. Sahoo, N.S. Parihar, B.N. Sharma, V. D. Kale, R.V. Nakat, A.R. Walunj, S. Mohapatra, A.K. Ahuja, D. Sharma, G. Singh, R. Noniwal, S. Devi, Residual behavior and risk assessment of flubendiamide on tomato at different agro-climatic conditions in India, Environ. Monit. Assess. 186 (11) (2014) 7673–7682, https://doi.org/10.1007/s10661-014-3958-4.

[5] W. Ma, J. Li, X. Li, H. Liu, Enrichment of diamide insecticides from environmental water samples using metal-organic frameworks as adsorbents for determination by liquid chromatography tandem mass spectrometry, J. Hazard Mater. 422 (2022) 126839, https://doi.org/10.1016/j.jhazmat.2021.126839.

[6] M. Pastor-Belda, I. Garrido, N. Campillo, P. Viñas, P. Hellín, P. Flores, J. Fenoll, Dispersive liquid–liquid microextraction for the determination of new generation pesticides in soils by liquid chromatography and tandem mass spectrometry, J. Chromatogr. A 1394 (2015) 1–8, https://doi.org/10.1016/j.chroma.2015.03.032.

[7] R. Kaur, K. Mandal, S.K. Sahoo, R. Kumar, R. Arora, B. Singh, Estimation and risk assessment of flubendiamide on fodder berseem clover (Trifolium alexandrinum L.) by QuEChERS methodology and LC-MS/MS, Environ. Sci. Pollut. Res. 23 (10) (2016) 9791–9798, https://doi.org/10.1007/s11356-016-6109-3.

[8] Z. Lu, Z. Zhang, N. Fang, Z. Hou, Y. Li, Z. Lu, Simultaneous determination of five diamide insecticides in food matrices using carbon nanotube multiplug filtration cleanup and ultrahigh-performance liquid chromatography–tandem mass spectrometry, J. Agric. Food Chem. 67 (39) (2019) 10977–10983, https://doi.org/10.1021/acs.jafc.9b02806.

[9] T. Schwarz, T.A. Snow, C.J. Santee, C.C. Mulligan, T. Class, M.P. Wadsley, S. C. Nanita, QuEChERS multiresidue method validation and mass spectrometric assessment for the novel anthranilic diamide insecticides chlorantraniliprole and Cyantraniliprole, J. Agric. Food Chem. 59 (3) (2010) 814–821, https://doi.org/10.1021/jf103468d.

[10] A. Kar, K. Mandal, B. Singh, Decontamination of chlorantraniliprole residues on cabbage and cauliflower through household processing methods, Bull. Environ. Contam. Toxicol. 88 (4) (2012) 501–506, https://doi.org/10.1007/s00128-012-0534-x.

[11] F.M. Malhat, Determination of chlorantraniliprole residues in grape by high-performance liquid chromatography, Anal. Methods 5 (6) (2012) 1492–1496, https://doi.org/10.1007/s12161-012-9400-z.

[12] F. Tian, C. Qiao, J. Luo, L. Guo, T. Pang, R. Pang, J. Li, C. Wang, R. Wang, H. Xie, Development and validation of a method for the analysis of five diamide insecticides in edible mushrooms using modified QuEChERS and HPLC-MS/MS, Food Chem. 333 (2020) 127468, https://doi.org/10.1016/j.foodchem.2020.127468.

[13] J. Fonseca, T. Gong, L. Jiao, H.-L. Jiang, Metal–organic frameworks (MOFs) beyond crystallinity: amorphous MOFs, MOF liquids and MOF glasses, J. Mater. Chem. A 9 (17) (2021) 10562–10611, https://doi.org/10.1039/d1ta01043c.

[14] Z. Hasan, S.H. Jhung, Removal of hazardous organics from water using metal-organic frameworks (MOFs): plausible mechanisms for selective adsorptions, J. Hazard Mater. 283 (2015) 329–339, https://doi.org/10.1016/j.jhazmat.2014.09.046.

[15] L. Li, J. Han, X. Huang, S. Qiu, X. Liu, L. Liu, M. Zhao, J. Qu, J. Zou, J. Zhang, Organic pollutants removal from aqueous solutions using metal-organic frameworks (MOFs) as adsorbents: a review, J. Environ. Chem. Eng. 11 (6) (2023), https://doi.org/10.1016/j.jece.2023.111217.

[16] N. Stock, S. Biswas, Synthesis of metal-organic frameworks (MOFs): routes to various MOF topologies, morphologies, and composites, Chem. Rev. 112 (2) (2011) 933–969.

[17] Y. Jiang, P. Ma, H. Piao, Z. Qin, S. Tao, Y. Sun, X. Wang, D. Song, Solid-phase microextraction of triazine herbicides via cellulose paper coated with a metal-organic framework of type MIL-101(Cr), and their quantitation by HPLC-MS, Microchim. Acta 186 (11) (2019), https://doi.org/10.1007/s00604-019-3889-4.

[18] J. Li, Y. Jiang, J. Yang, Y. Sun, P. Ma, D. Song, Fabrication of the metal-organic framework membrane with excellent adsorption properties for paraben based on micro fibrillated cellulose, Chem. Res. Chin. Univ. 38 (3) (2022) 790–797, https://doi.org/10.1007/s40242-022-1511-5.

[19] W. Ma, L. Xu, X. Li, S. Shen, M. Wu, Y. Bai, H. Liu, Cysteine-functionalized metal–organic framework: facile synthesis and high efficient enrichment of N-linked glycopeptides in cell lysate, ACS Appl. Mater. Interfaces 9 (23) (2017) 19562–19568, https://doi.org/10.1021/acsami.7b02853.

[20] Y. Dong, J. Zheng, J. Xing, T. Zhao, S. Peng, In situ synthesis of gold nanoparticle on MIL-101(Cr)-NH2 for non-enzymatic dopamine sensing, Colloids Surf. A Physicochem. Eng. Asp. 650 (2022) 129618, https://doi.org/10.1016/j.colsurfa.2022.129618.

[21] Z. Chang, B. He, X. Gong, X. Qi, K. Liu, Cr-based metal–organic frameworks (MOFs) with high adsorption selectivity and recyclability for Au (III): adsorption behavior and mechanism study, Sep. Purif. Technol. 325 (2023) 124612, https://doi.org/10.1016/j.seppur.2023.124612.

[22] X. Liu, W. Cheng, Y. Yu, S. Jiang, Y. Xu, E. Zong, Magnetic ZrO2/PEI/Fe3O4 functionalized MWCNTs composite with enhanced phosphate removal performance and easy separability, Compos. B Eng. 237 (2022) 109861, https://doi.org/10.1016/j.compositesb.2022.109861.

[23] X. He, X. Fan, W. Feng, Y. Chen, T. Guo, F. Wang, J. Liu, K. Tang, Incorporation of microfibrillated cellulose into collagen-hydroxyapatite scaffold for bone tissue engineering, J. Biol. Macromol. 115 (2018) 385–392, https://doi.org/10.1016/j.ijbiomac.2018.04.085.

[24] X.-L. Song, H. Lv, K.-C. Liao, D.-D. Wang, G.-M. Li, Y.-Y. Wu, Q.-Y. Chen, Y. Chen, Application of magnetic carbon nanotube composite nanospheres in magnetic solid-phase extraction of trace perfluoroalkyl substances from environmental water samples, Talanta 253 (2023), https://doi.org/10.1016/j.talanta.2022.123930.

[25] Z. Xiao, M. He, B. Chen, B. Hu, Polydimethylsiloxane/metal-organic frameworks coated stir bar sorptive extraction coupled to gas chromatography-flame photometric detection for the determination of organophosphorus pesticides in

environmental water samples, Talanta 156–157 (2016) 126–133, https://doi.org/10.1016/j.talanta.2016.05.001.

[26] S. Wang, S. Hou, C. Wu, Y. Zhao, X. Ma, RuCl3 anchored onto post-synthetic modification MIL-101(Cr)-NH2 as heterogeneous catalyst for hydrogenation of CO2 to formic acid, Chin. Chem. Lett. 30 (2) (2019) 398–402, https://doi.org/10.1016/j.cclet.2018.06.021.

[27] A. Ghiasi, A. Malekpour, S. Mahpishanian, Aptamer functionalized magnetic metal–organic framework MIL-101(Cr)-NH2 for specific extraction of acetamiprid from fruit juice and water samples, Food Chem. 382 (2022) 132218, https://doi.org/10.1016/j.foodchem.2022.132218.